EDDA internal report 95-04

Determining COSY Beam Parameters from Elastic Proton-Proton Scattering

H. Rohdjeß
ISKP,Universität Bonn
E-Mail: rohdjess@iskp.uni-bonn.de
Tel.: (0228) 73-2506
FAX.: (0228) 73-2505

December 13, 1995

Abstract

The reaction vertex for proton-proton elastic events is reconstructed from the azimuthal angles as measured with the EDDA detector, a segmented, cylindrically symmetric scintillator detector. By exploiting the coplanarity of the two ejectiles the mean and width of the vertex distribution and the angle of the COSY beam at TP2 are extracted. The analysis procedure is explained and the result for various running periods (November 1994, March and September 1995) are presented.

Contents

1 Overview

The EDDA Detector measures the point of interception of the two final-state particles of proton-proton scattering events with a cylindrical symmetric scintillator array around the COSY beam pipe. Two-body kinematics require the two prongs to be coplanar with the beam. Thus deviations from coplanarity of proton-proton scattering events with the detector symmetry axis bear information on the position and angle of the COSY beam axis with respect to the detector. The method employed is an extended and refined version of the one described in [1].

Since the detector position is unchanged when the COSY beam is ramped, shifts of the beam position and angle during beam acceleration can be measured.

Notation

If not stated otherwise all quantities are given in the EDDA coordinate system, i.e. x points outboard, y up, and z downstream from the EDDA target position at TP2.

Widths given as standard deviation are denoted by σ, while δ signifies FWHM (full width at half maximum)

y_b	fiber target position in y at z=0.
x_b	beam position in x at z=0 and y_b.
x'_b	horizontal beam angle (dx/ds) at z=0.
y'_b	vertical beam angle (dy/ds) at z=0.
$\delta x_{b,FWHM}$	size of the beam in x at z=0 and y_b.
$\delta y_{b,FWHM}$	vertical size of the target.
$\delta\phi$	resolution in the azimuthal angle ϕ of the EDDA detector (1.8° [1])
R	mean radius of the EDDA slab layer (164mm)

2 The Method

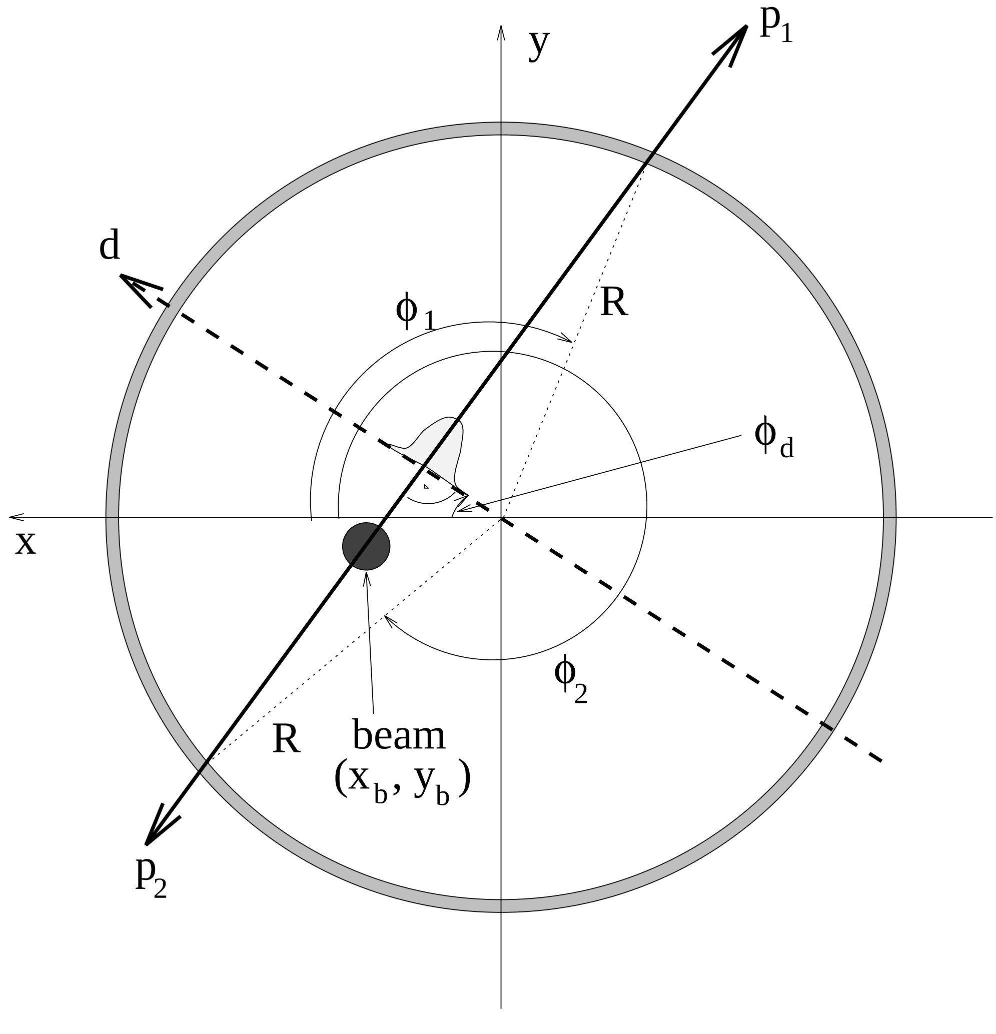

Figure 2.1: Geometry for a beam parallel to the detector symmetry axis z as explained in the text.

For simplicity the analysis method will first be described for a beam parallel to the detector symmetry axis, the generalization to tilted beams will be the topic of Section 2.2

2.1 Beam Parallel to the Detector Axis

Consider a beam displaced by (x_b,y_b) in the x,y-plane from the detector symmetry axis. In a projection on the x,y-plane of an elastic scattering event (prongs p_1 and p_2 in Fig. 2.1) a beam displacement leads to a deviation from coplanarity when the vertex *is assumed* to be at (x,y)=(0,0) (dotted lines).

The EDDA detector measures the point of interception of these two prongs with the slab layer at $R = 164$mm. Connecting these two points by a straight line the distance to the origin of the coordinate system is a function of the beam position. If we now define an axis $\vec{d}$ perpendicular to this line (fat line in Fig. 2.1) we can calculate the angle of the $\vec{d}$ axis to the x-axis

$$\phi_d = \frac{\phi_1 + \phi_2}{2} \tag{2.1}$$

and the position d along this axis:

$$d = -R \cos \frac{\phi_1 - \phi_2}{2} \tag{2.2}$$

The orientation of the $\vec{d}$ axis has been chosen to point to the "left", to the effect that $\phi_d \in [-\pi/2, \pi/2]$ must be forced by adding or subtracting π from the expression given in Eq. 2.1. The negative sign in Eq. 2.2 is due to this choice. Eqs. 2.1 and 2.2 are an eventwise transformation of (ϕ_1,ϕ_2) into(d,ϕ_d).

The connection between d and the beam position is evident. Using basic trigonometric relations (For a derivation see Appendix A) one derives:

$$d = x_b \cos \phi_d + y_b \sin \phi_d \tag{2.3}$$

(Hint: this relation is easy to see when you consider x_b=0 or y_b= 0 in Fig. 2.1.) Now, the idea is to combine events with different ϕ_d to disentangle the influence of x_b and y_b on d.

2.1.1 Experimental Input

Elastic scattering events are selected through the following criteria: (for details cf. [1] for example)

- A perfect hit pattern in the detector is required (one cluster of semi-rings on either side of the detector and two matching clusters in the slabs, 211 in Bonn notation).
- A kinematic deficit (π minus the folding angle between the two prongs in the c.m. system, should be 0 for a perfect pp-elastic event) below 7.5°.
- Off all final spectra the contribution from the carbon contents of the CH_2 target is subtracted (cf. [1] for example).

For each event ϕ_d and d are calculated. The events are sorted into spectra according to their ϕ_d value. Events with $|\phi_d| < 10°$ are discarded because event reconstruction may be erroneous due to the overlap of the semirings at y≈ ±R, x≈0.

A d-distribution is accumulated for 16 ϕ_d-intervals from -90° to -10° and 10° to 90°, each 5° wide. These 16 spectra are the input to the analysis.

When the time dependence of beam parameters is investigated these spectra are accumulated for small time intervals, usually 25, 50 or 100ms wide, i.e. for each time interval 16 spectra are generated.

2.1.2 Fit Procedure

The experimental d-distributions are of gaussian shape. After the integral of each d-spectrum was normalized to one, they can be fitted by a gaussian

$$n(d) = \frac{1}{\sqrt{2\pi}\sigma_d} \exp\left(-\frac{(d-\bar{d})^2}{\sigma_d{}^2}\right) \tag{2.4}$$

with two fit parameters $\bar{d}$ and σ_d. dscalesimple For a given ϕ_d these parameters are identified with (cf. Appendix A):

$$\bar{d} = x_b \cos\phi_d + y_b \sin\phi_d \tag{2.5}$$

and

$$\sigma_d = \sqrt{\cos^2\phi_d \sigma_{x_b}^2 + \frac{R^2}{2}\sigma_\phi^2} \tag{2.6}$$

The vertical size of the target is negligible small and has been set to 0. Thus all 16 spectra are fitted by four fit parameters *simultaneously*: x_b, y_b, $\sigma_{x_b}^2$, and σ_ϕ^2. For the implementation of the fitting procedure the minimizer MIGRAD (variable metric method) of the CERN package MINUIT [2] is used.

2.1.3 First Results

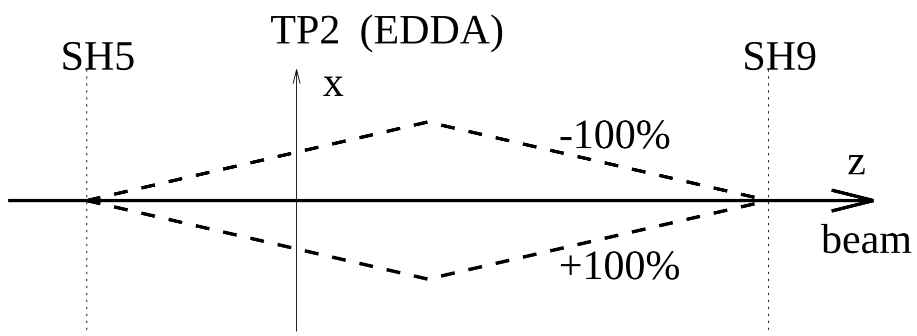

Figure 2.2: Sketch of the orbit distortion expected for a simultaneous excitation of the horizontal steerers SH5 and SH9. The beam position is measured by EDDA at TP2.

As a test of the sensitivity of the method data acquired in September 95 is taken. Here in the flattop, i.e. at constant energy, two steerers around the EDDA target region where excited to produce a horizontal excursion of the beam (a “bump”). The geometry is shown in Fig. 2.2. The strength of the magnets (originally at 0%) was ramped within 100ms to +100%, then, after 10ms, they were ramped linearly to -100% within 1000ms and finally –after another 10ms– brought back to 0% within 100ms.

The result of the fit (Fig. 2.3) shows the response of the beam: The beam position x_b follows closely the strength of the magnet. The vertical target position y_b, the beam width $\delta x_{b,FWHM}$, and the angular resolution $\delta\phi$ remain basically unchanged. Obviously, *the method is sensitive to changes in the beam position!*.

Another test is to take data taken at fixed energy and to observe the increase in beam size due to the emittance growth when the beam is “heated” by the target. The result of the fit is

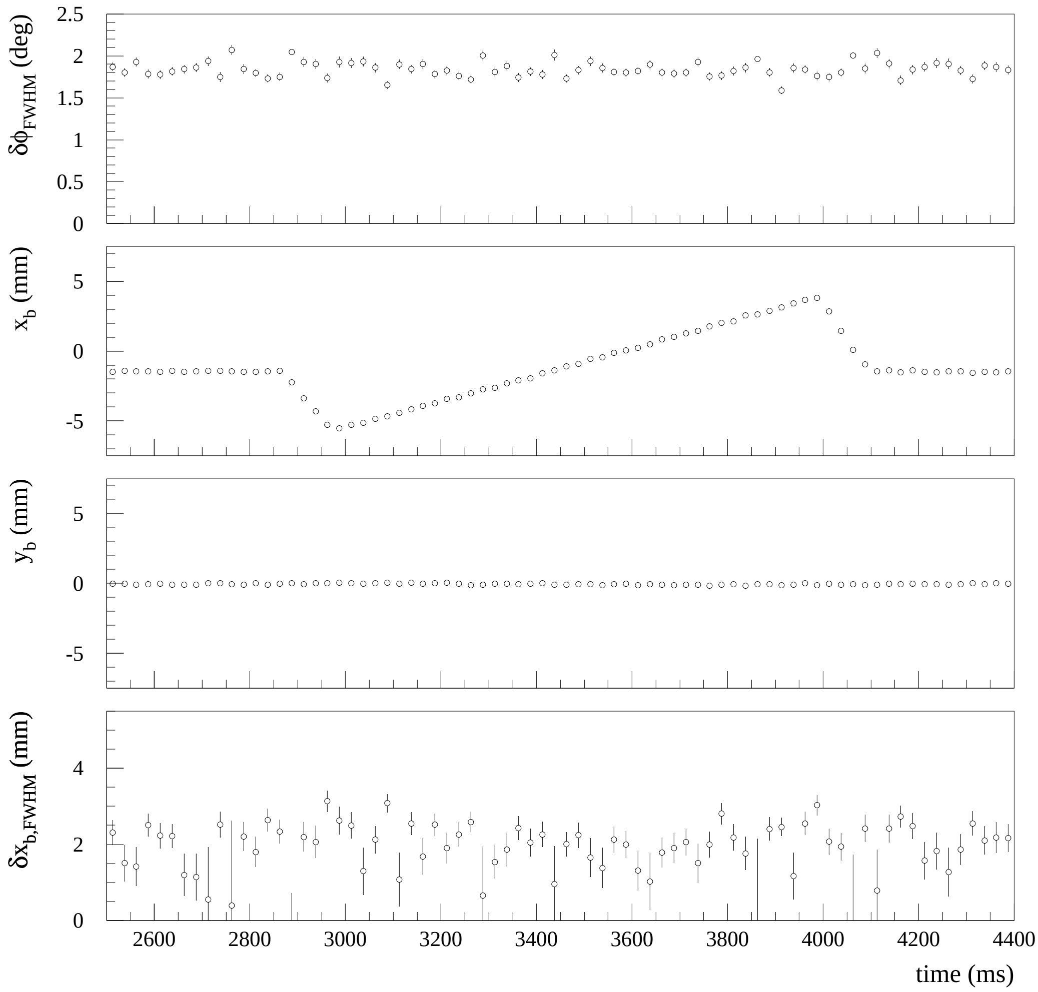

Figure 2.3: Result of the fit for flattop data at 3400MeV/c (September 95) where around 3000-4000ms a horizontal excursion of the beam was produced by exciting steerer magnets (cf. Fig. 2.2). (25ms bins in time).

shown in Fig. 2.4. As expected only the beam size increases with time. All other parameters remain constant. It is interesting to see, that even the overshoot of the target before it settles at the correct height is resolved. We conclude: *one can also extract the beam width!*

A discussion of statistical and systematic errors and a discussion of the sensitivity of the fit to different fit parameters will be given in Section 4.

2.2 Tilted Beam

In the previous section it has been assumed that the beam is parallel to the symmetry axis of the detector. This is not necessarily true. In general, the beam may be tilted with respect to

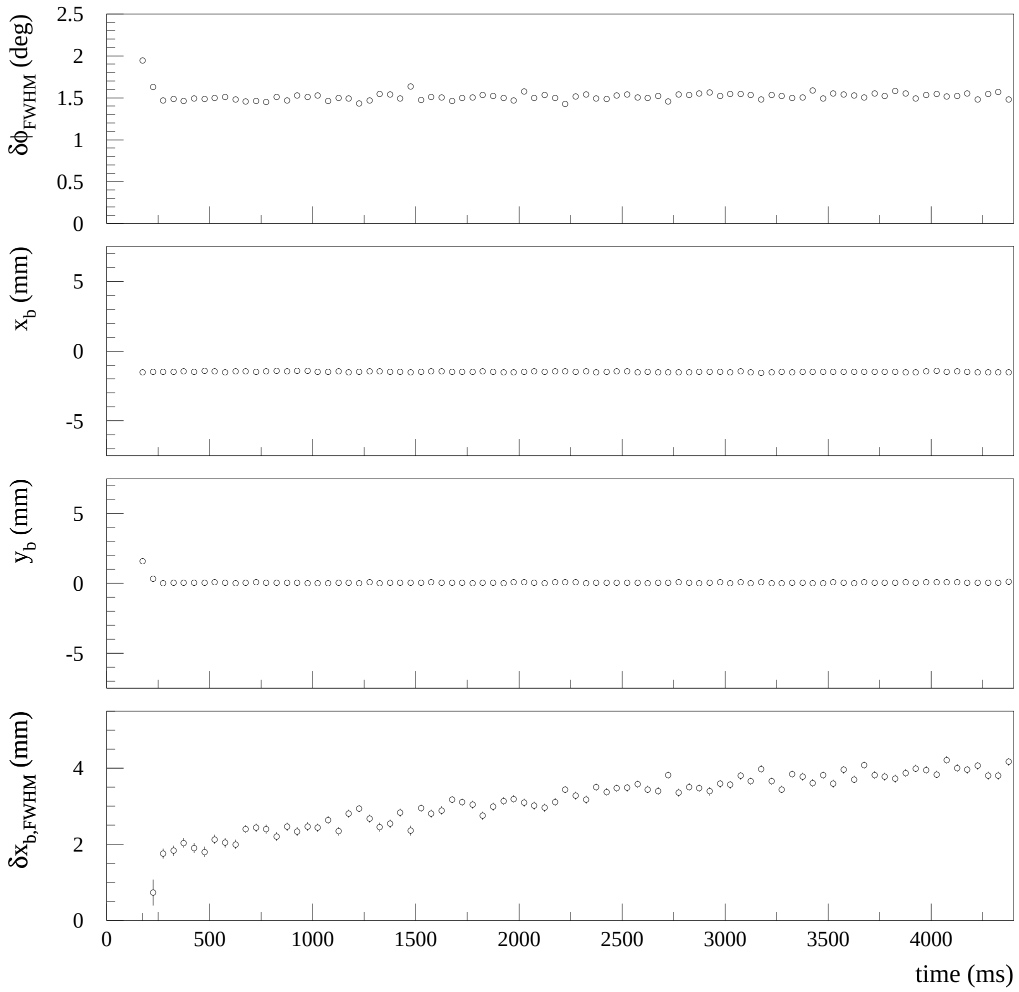

Figure 2.4: Result of the fit for flattop data at 2250MeV/c (September 95). The fiber target starts to move at 0ms and reaches the beam position around 250ms. (50ms wide bins in time).

the detector both horizontally and vertically, described by the parameters x'_b and y'_b. Fig. 2.5 shows that a tilted, non-displaced beam mocks up a beam displacement in the previous analysis: since only the azimuthal angles are considered we reconstruct the event in a plane parallel to the detector z-axis defined by the two points of interception with the EDDA detector (dark plane in Fig. 2.5). The reaction plane (light plane in Fig. 2.5) is defined by the same two points but must be coplanar to the beam. Consider a pp-elastic event where the two protons are emitted up-down: if the beam angle x'_b is positive the two protons tracks will be displaced to the left with respect to their origin. The displacement depends on the distance in z they travel until they hit the EDDA slab layer at radius R. As evinced in Fig. 2.5 the line through the two points of interception projected into the x-y plane looks as if the beam were displaced to positive x.

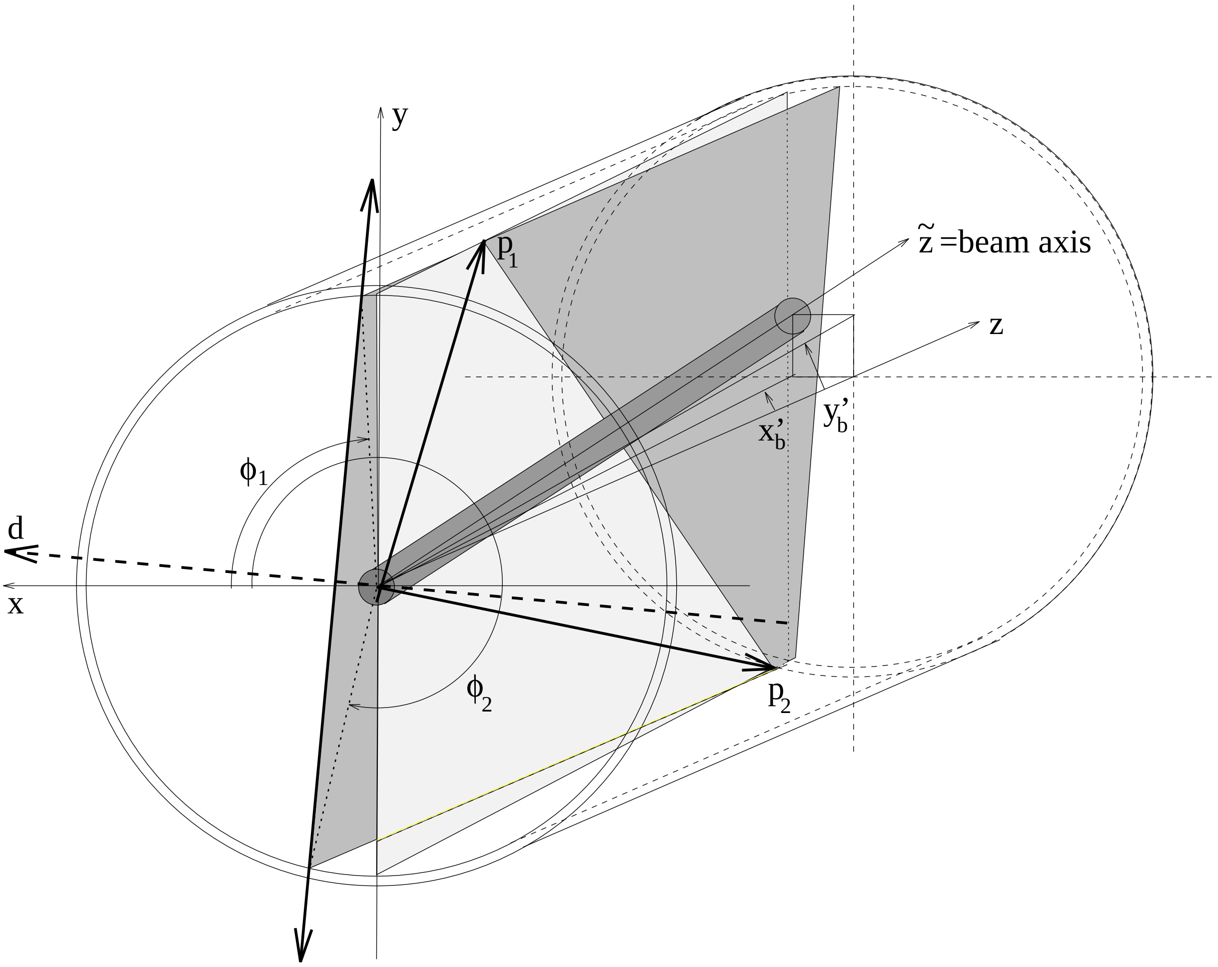

Figure 2.5: Geometry for a tilted beam (axis $\tilde{z}$ tilted by x_b', y_b') as explained in the text.

In Appendix A it is derived that the measured value of d of a tilted beam is given by:

$$d = (x_b + \frac{z_1 + z_2}{2} x_b') \cos \phi_d + (y_b + \frac{z_1 + z_2}{2} y_b') \sin \phi_d \tag{2.7}$$

and reduces to Eq. 2.3 for x_b'=y_b'=0. z_1 and z_2 are the z-coordinate of the point where the tracks of the proton intercept the EDDA slab layer. Evidently, the parameters x_b and x_b' (as y_b and y_b') are strongly correlated and can only be distinguished by considering events with different $z_1 + z_2$. For pp-elastic scattering the correlation of the two z values as a function of beam kinetic energy T_p is given by:

$$z_1 z_2 = R^2 \gamma^2 = R^2 (1 + \frac{T_p}{2m_p}) \tag{2.8}$$

where m_p is the proton mass. Thus symmetric events ($z_1 = z_2$) with $z_1 + z_2 = 2R\gamma \approx 400$mm are less sensitive to x_b' and y_b' than asymmetric events ($z_1 = z_{\max} = 1$m) with $z_1 + z_2 \approx 1100$mm

2.2.1 Experimental Input

For each calculated ϕ_d the data was subdivided into 14 classes with respect to their $z_1 + z_2$, ranging from 400 to 1100 mm, each 50mm wide. For a given energy only those classes were

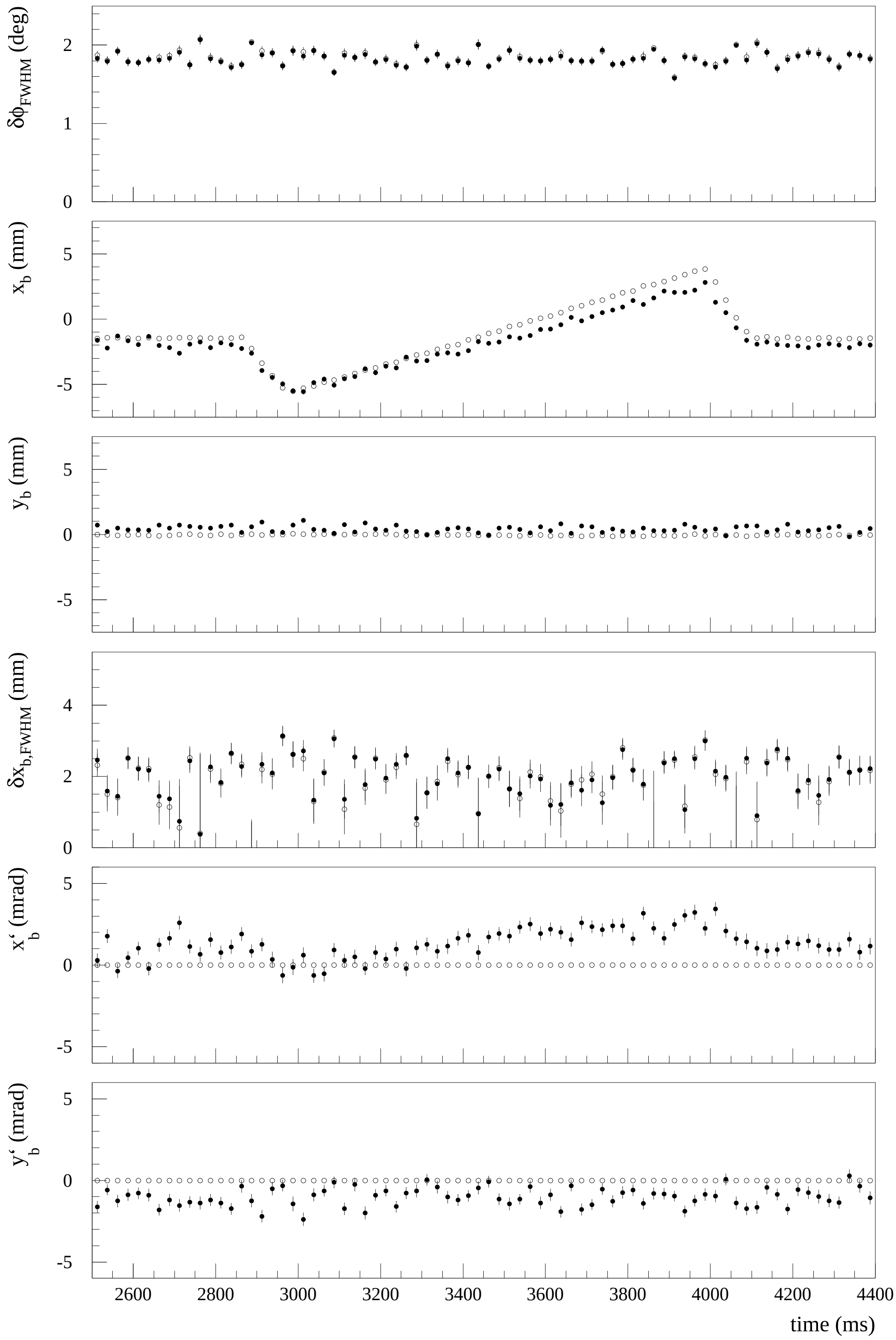

Figure 2.6: Result of the fit for flattop data at 3400MeV/c (September 95, same data as in Fig. 2.3). The solid symbols are the result of the fit when the beam angles x'_b and y'_b are included in the fit. Th open symbols are the data as in Fig. 2.3).

included in the fit where the kinematics allowed for the respective $z_1 + z_2$ value. Usually 8-13 classes are useful, and for each of these 16 d distributions for the different ϕ_d ranges are sorted. The resulting 128-208 spectra are fitted *simultaneously* with six parameters x_b, y_b, σ_ϕ, σx_b, x'_b, and y'_b.

2.2.2 First Results

The result of the fit (same data as in Fig. 2.3) is shown as the solid symbols in Fig. 2.6. The change in beam angle and the beam position have the same sign as one expects for the geometry shown in Fig. 2.2. The total change in angle during the bump (4mrad) and the range of the beam position shift (8mm) yield a distance of the origin of the beam rotation at -2m with respect to TP2 which agrees rather well with the distance of the steerer magnet SH5 to TP2 (1.75m). The fact that the change in x_b and x'_b have the same sign indicates that the method is indeed sensitive to changes in beam angles, since Eq. 2.7 implies that these parameters are *anticorrelated* when the change would be an artefact of the fitting procedure.

3 Results and Discussion

Prior to examining the sensitivity of the method, the possible correlation of fit parameters and the interpretation of the errors of the fit I will present the result of the fit applied to data taken during the ramp. Figs. 3.1-3.3 show the shift in horizontal beam position and width as well as beam angles for data samples taken in

1. November 1994: Runs 135-179,181-207 (CH_2 Target) 211-247 (C Target).
2. March 1995: Runs 136-181 (CH_2 Target) 119-135 (C Target).
3. September 1995: Runs 846-875 (CH_2 Target) 812-831 (C Target).

For comparison both the beam momentum and the response of the secondary electron monitor (SEM) as a measure of the luminosity are plotted. At the bottom of Figs. 3.1-3.3 the χ^2 per datapoint of the fit is shown. The *absolute* value of the χ^2 is meaningless since it depends on d-range included in the fit (extending the d-range adds a lot of data points with a contents of 0 counts which are perfectly fitted and reduce the χ^2. Taking all bins with zero counts out of the fit leads to too large widths when the statistics per d-distribution is low).

In November 94 (Fig. 3.1) the beam position stayed rather stable throughout the ramp, some shifts in the beam angle x'_b is seen, especially in the transition to the flattop. Most strikingly the rise in the SEM signal coincides with a dramatic increase in the horizontal beam width. Beam profile measurements showed a correlated *decrease* of the vertical beam width. Thus, the increase in luminosity on the horizontally mounted EDDA fiber target is due to a change of shape of the beam ellipse at TP2.

The March 95 data (Fig. 3.2) shows strong oscillations of the horizontal beam angle and position, especially between 1000 and 2000ms. During this time the so-called "backlag windings" of the COSY-11 dipole (This coil is intended to compensate for changes of the magnetic field due to the vacuum chamber of the COSY-11 experiment relative to the other dipoles) were turned on and off to compensate beam losses (cf. EDDA log#2 p.19).

Finally in September 95 both the beam position, width, and angle stayed rather constant, with the beam moving slowly outward with time. The "bump" in the flattop has been discussed earlier in this report.

All these results have in common:

- the quality of the fit is enhanced when the angle of the beam x'_b and y'_b are varied in the fit (reduction of the χ^2).
- the change in the horizontal beam position and the horizontal beam angle are anticorrelated. This is not surprising because the last quadrupole-multiplet of COSY upstream of TP2 focuses the beam, such that deviation of the beam orbit from the symmetry-axis of these quadrupoles result in an angle with opposite sign at TP2 when the beam waist is somewhat downstream from TP2.
- the angular resolution ($\propto 1/\delta\phi$) slowly decreases with energy. This is explained by smaller energy deposits at higher beam energies which introduce larger statistical fluctuations in the measured charge. However, it stays in the correct order of magnitude (cf. [1]).

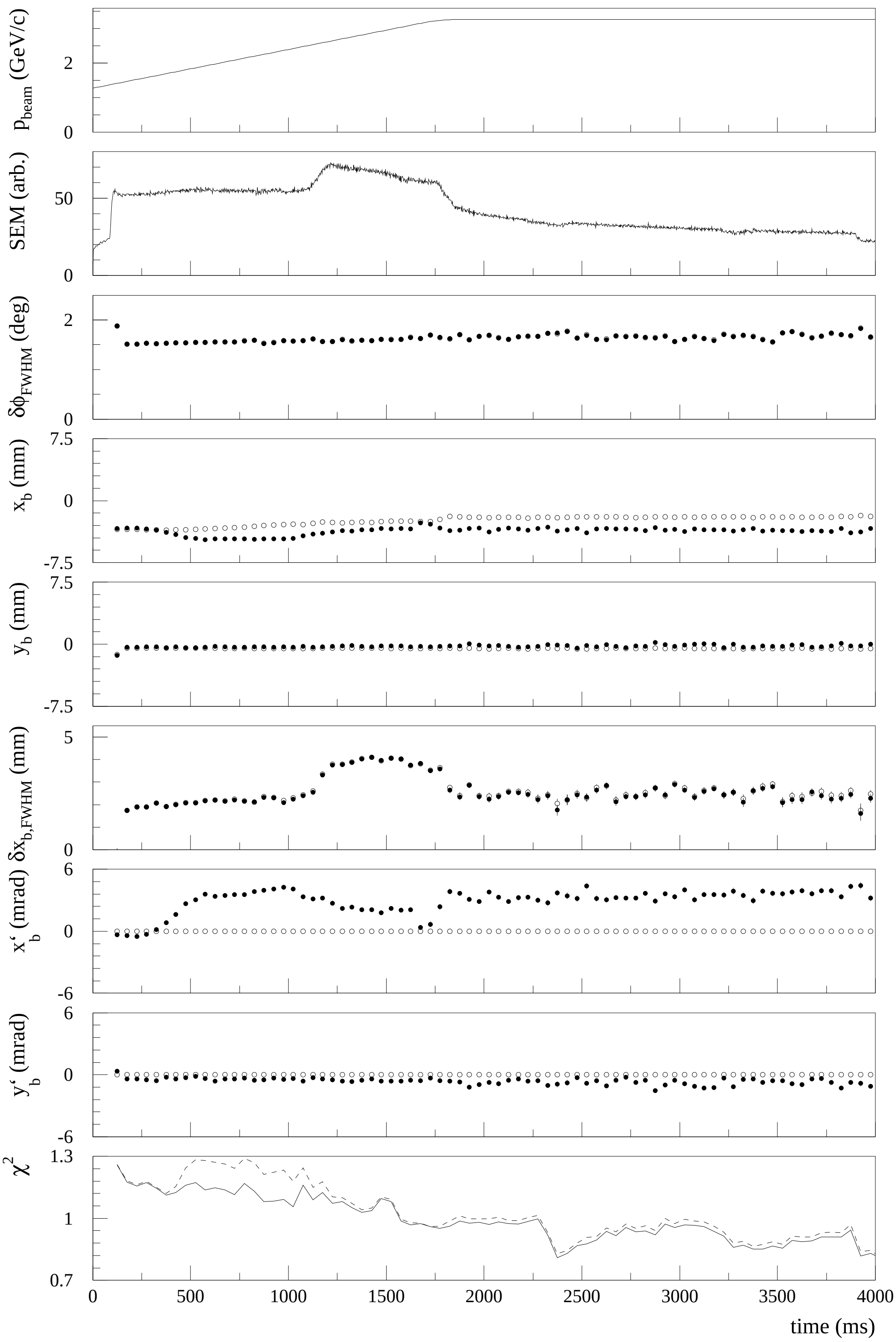

Figure 3.1: Fit parameter as a function of time (November 1994 data). Also shown is the momentum of the beam and the signal of the secondary electron monitor (SEM). Solid (open) symbols and solid (dashed) lines show the result of the fit when x_b' and y_b' were (were not) included as fit parameters. (50ms time bins).

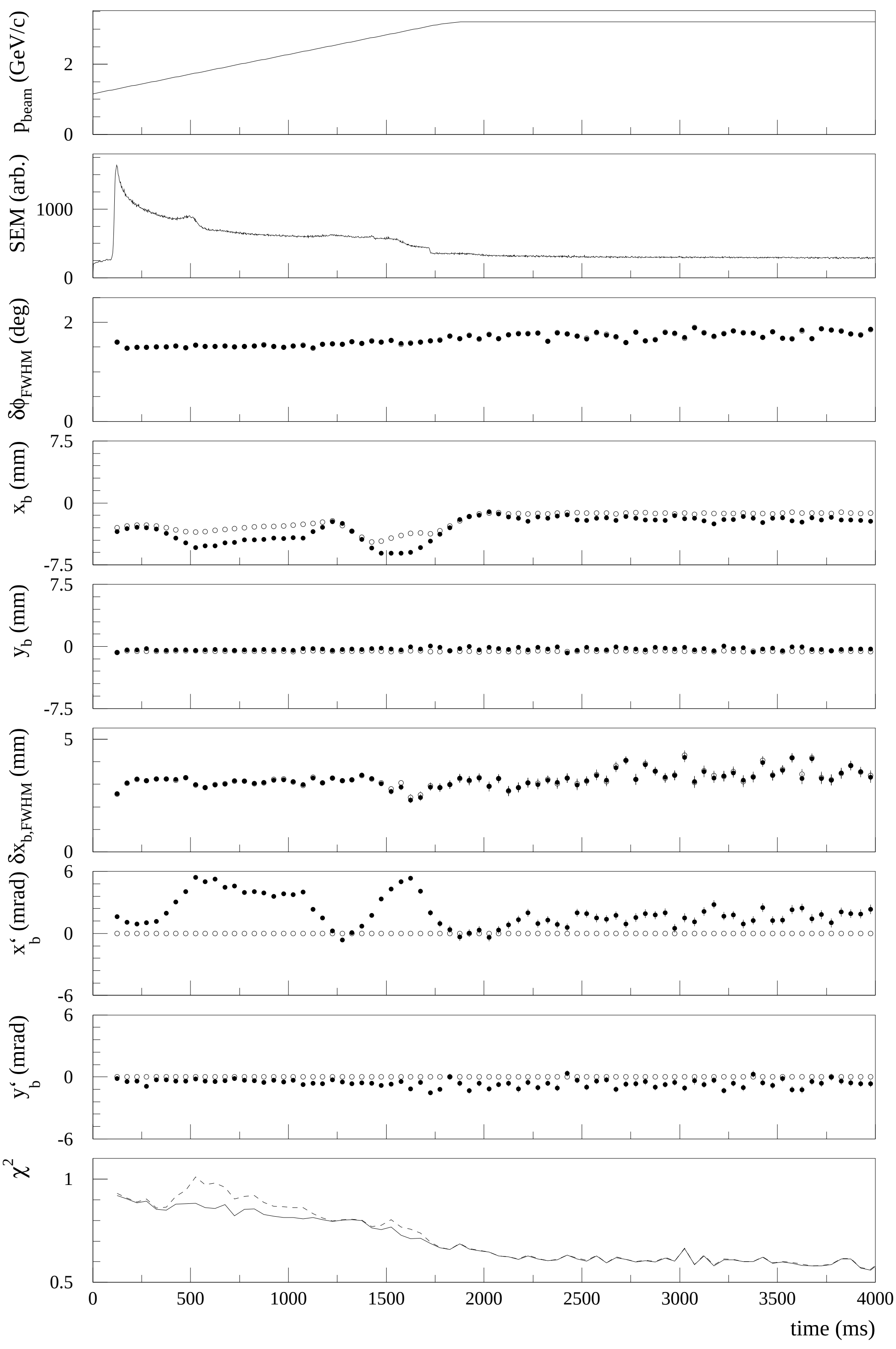

Figure 3.2: Fit parameter as a function of time (March 1995 data). Also shown is the momentum of the beam and the signal of the secondary electron monitor (SEM). Solid (open) symbols and solid (dashed) lines show the result of the fit when x'_b and y'_b were (were not) included as fit parameters. (50ms time bins).

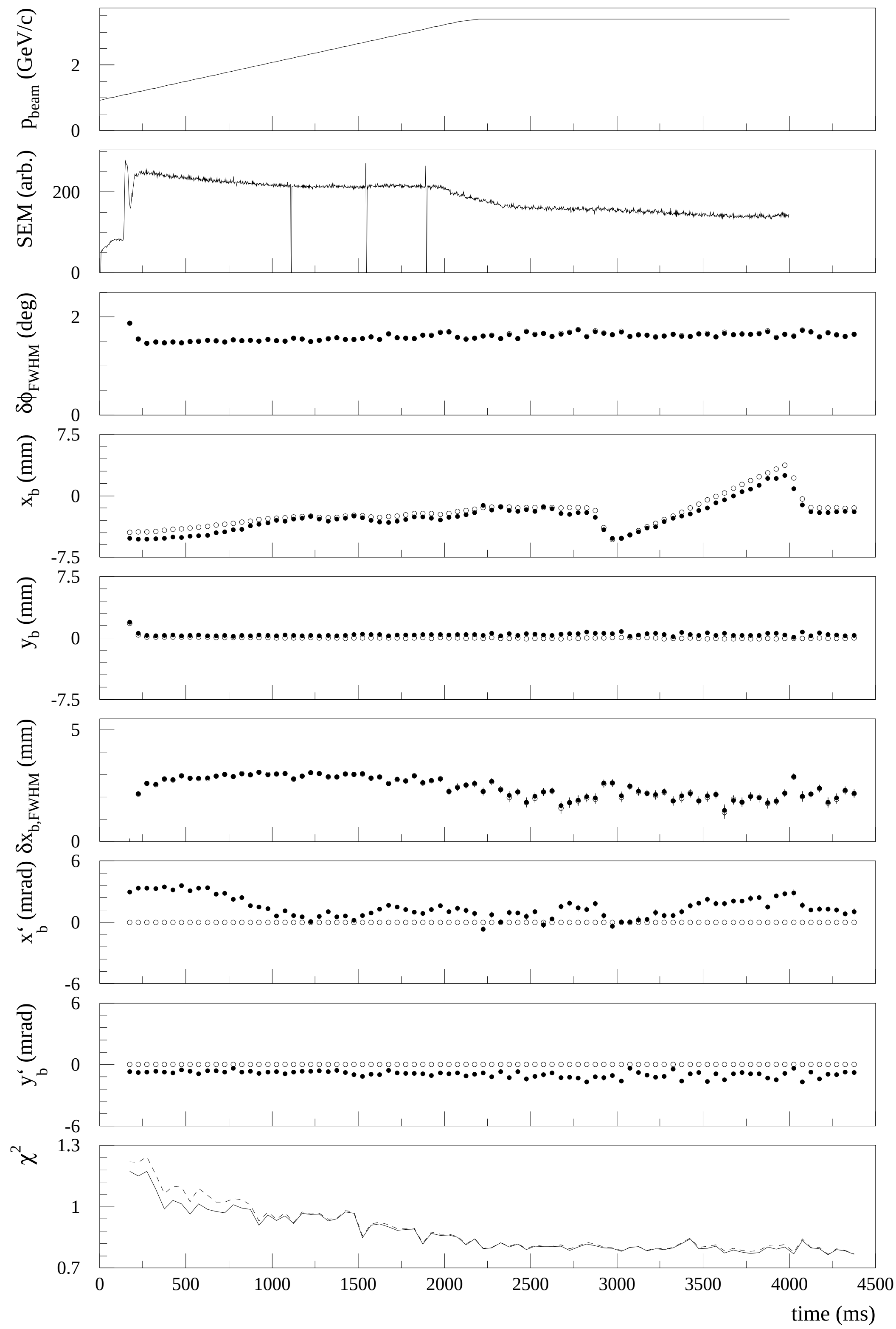

Figure 3.3: Fit parameter as a function of time (September 1995 data). Also shown is the momentum of the beam and the signal of the secondary electron monitor (SEM). Solid (open) symbols and solid (dashed) lines show the result of the fit when x_b' and y_b' were (were not) included as fit parameters. (50ms time bins).

The result of the fit for various data samples is available for public access on the World Wide Web [3].

4 Errors and Sensitivity of the Fit

All errors displayed in the previous figures are the errors of the fit which include – since they enter in the calculation of the χ^2 the statistical errors. The errors are calculated by MINUIT [2] and are standard deviations. The error of a fit parameter is calculated from the second-derivative matrix at the minimum (such that the gradient of the χ^2 function with respect to the fit parameters vanishes). The error of a parameter is the square root of the corresponding diagonal element of the inverted second-derivative matrix (for details see [2]). It contains the error due to correlation of fit parameter.

Correlation and Sensitivity of Fit Parameters

At the most six parameter are fitted: x_b, y_b, $\delta\phi$, $\delta x_{b,FWHM}$, x'_b, and y'_b. Of these always two are strongly correlated:

$\boxed{x_b \textbf{ and } x'_b}$ Both are sensitive to changes of the beam in the horizontal plane. They are anticorrelated. The correlation is evident when comparing Figs. 2.3 and 2.6: in the first x'_b was set to 0 and the fit errors in x_b are tiny. The errors – and the scatter of the fit results – is increased when x'_b is included in the fit. However, inclusion of the beam angles in the fit changes the beam position by at most 2mm, such that the latter is rather well determined.

$\boxed{y_b \textbf{ and } y'_b}$ The same holds true as for x_b and x'_b. Since we *know* that y_b stays constant with time, its change as a result of the fit is an estimate of the *systematic errors*.

$\boxed{\delta\phi \textbf{ and } \delta x_{b,FWHM}}$ Both parameter describe the horizontal width of the vertex distribution. $\delta x_{b,FWHM}$ is only distinguished by a different scaling with ϕ_d. The fit is sensitive to $\delta x_{b,FWHM}$ only when it is not much smaller than $R\delta\phi/\sqrt{2} \approx$ 3.6mm (cf. Eq. 2.6). Thus, $\delta x_{b,FWHM}$ is only poorly fitted whenever the beam width is much less than 3.6mm (FWHM). This is the reason why the errors on $\delta x_{b,FWHM}$ in Fig. 2.3 ($\delta x_{b,FWHM} \approx$ 2mm) are very large.

To visualize the sensitivity of the fit to various parameters some selected d-distributions (of typically 160) are displayed in Figs. 4.1-4.3:

- In Fig. 4.1 the variation of d with ϕ_d is shown, the sensitivity to a beam displacement is evident.
- The width is much harder to determine. Fig. 4.2 shows that even an increase of the width by a factor of 1.5 yields only a small change in the measured d distribution. In fact $\delta x_{b,FWHM}$ is only sensitive to the variation of this width with ϕ_d.
- Finally the beam angle only enters through a dependence of $\bar{d}$ on $z_1 + z_2$. In general, this effect is small and the relative error on x'_b and y'_b rather large (see Fig. 4.3).

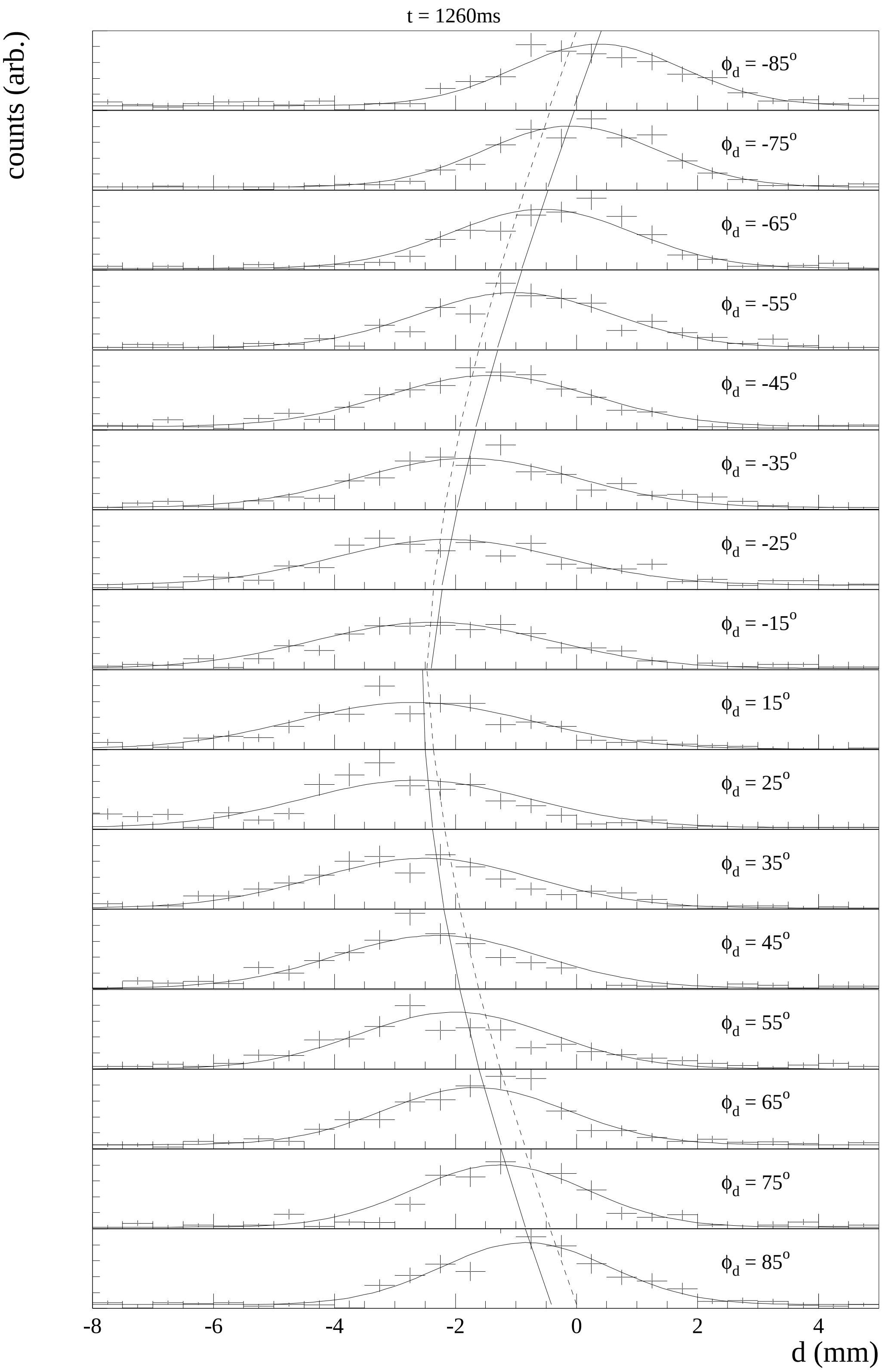

Figure 4.1: Fit to data taken in the ramp (run March 1995, cf. Fig. 3.2) at t=1260±50ms (≈2570MeV/c). The variation of the mean value for $\bar{d}$ with ϕ_d for a beam displacement x_b=–2.51mm, y_b=–0.41mm and angles close to 0 is shown. The solid gaussian is the fit to the data (crosses) and the solid line shows the variation of $\bar{d}$ with ϕ_d, the dashed line is calculated for y_b=0 and evinces the sensitivity to this parameter. The distributions were accumulated for $z_1 + z_2 = 975 \pm 25$mm.

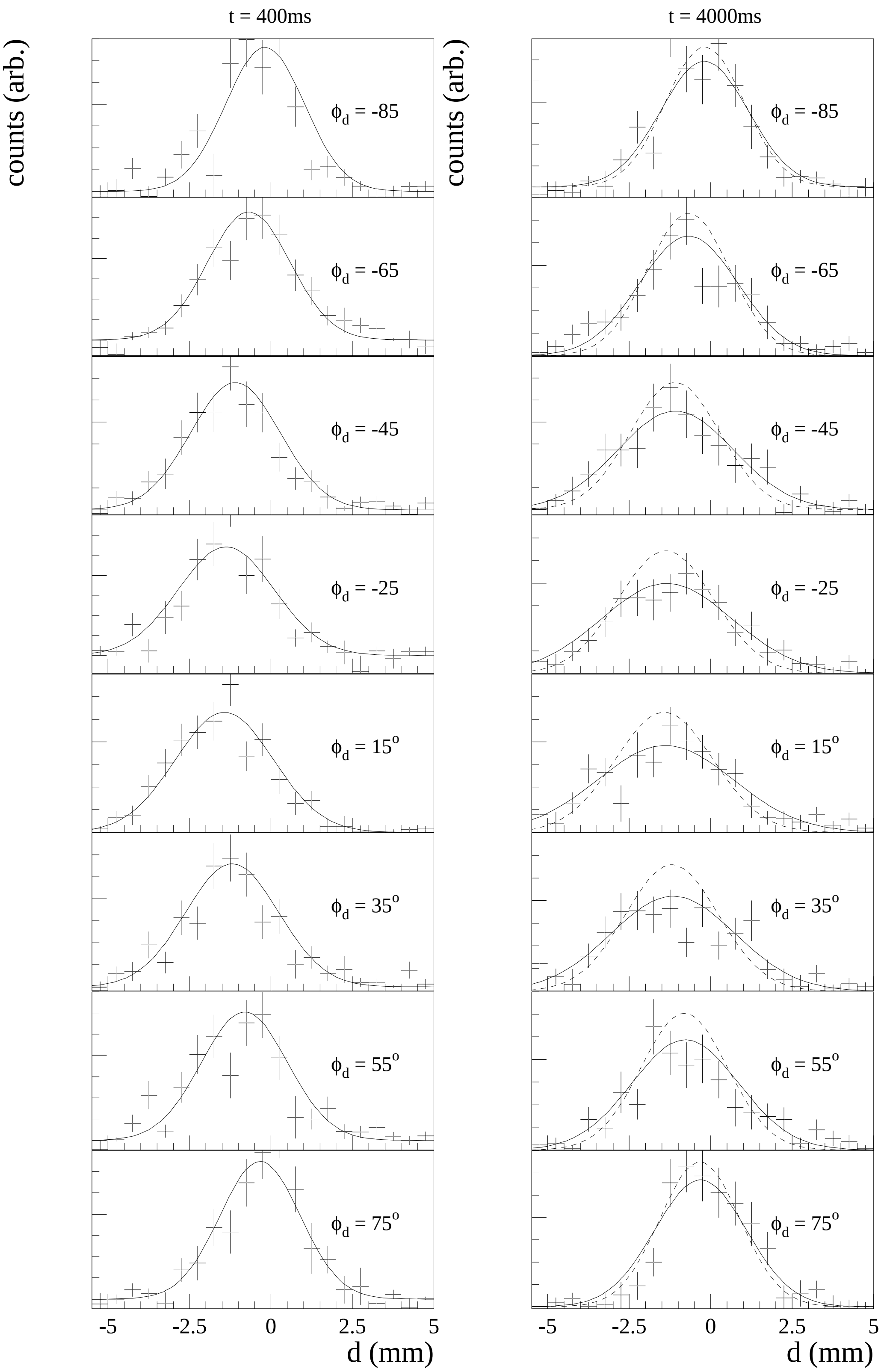

Figure 4.2: Fit to flattop data (run September 1995, beam momentum 2250 MeV/c, cf. Fig. 2.4) at two different times since "EDDA in" for the range $z_1 + z_2 = 775 \pm 25$mm and various angles ϕ_d. The left column (t=400ms) was fitted with a beam width $\delta x_{b,FWHM}$ of 2.19 ± 0.07mm and the right column (t=4000ms) with 3.84 ± 0.07mm. All other fit parameter are the same within their error. The fitted curve is the solid line. On the left the fit result for t=400ms is shown for comparison as the dashed line.

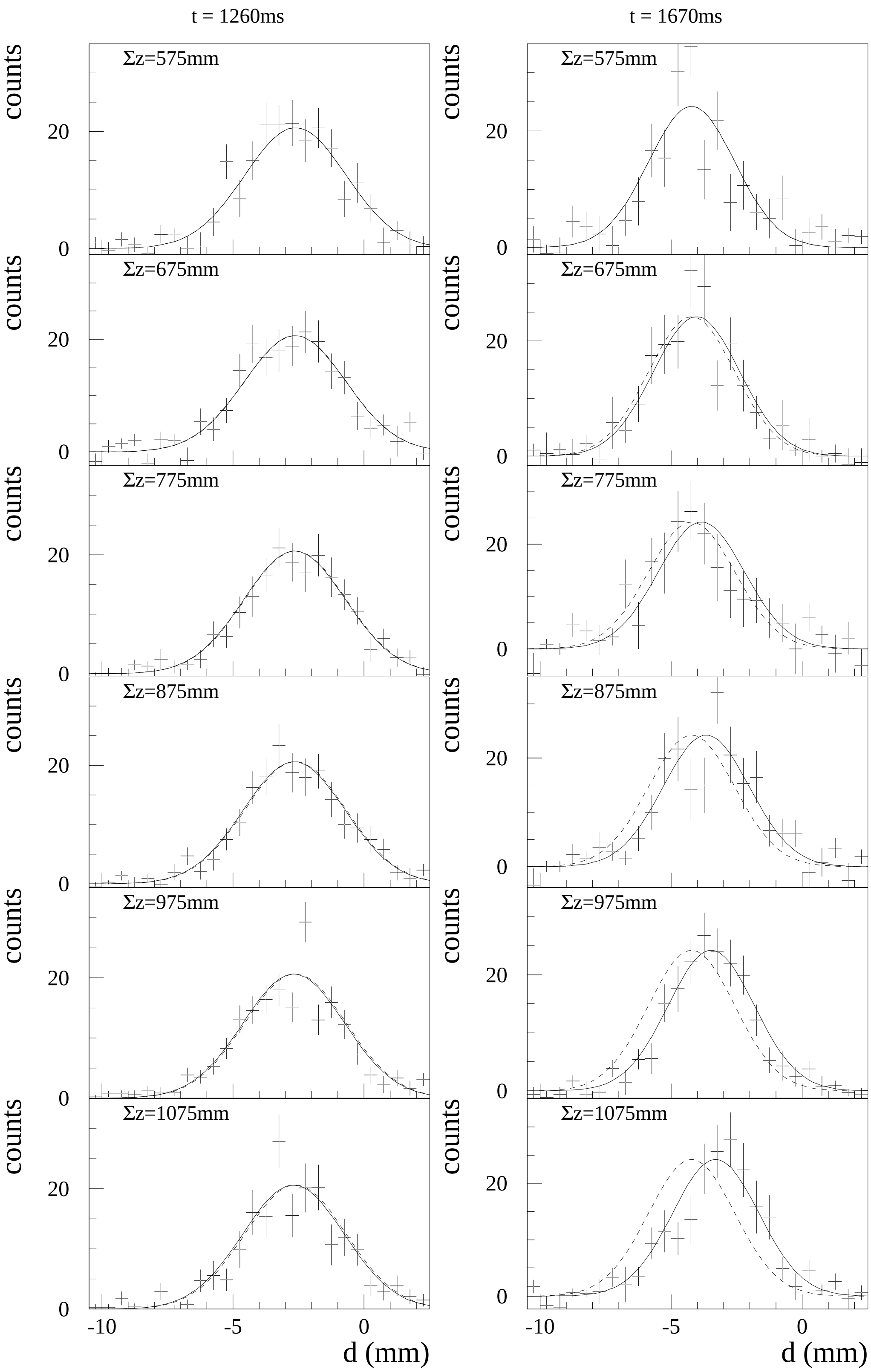

Figure 4.3: Fit to data taken in March 1995 (cf. Fig. 3.2) during the ramp at ϕ_d=15°. The two times were selected to show the sensitivity of the fit to x'_b. The left column shows the variation of the d-distribution with $\Sigma z = z_1 + z_2$ when a value of x'_b=0 was fitted, the right shows the same at another time where the fit yields x'_b= 5mrad.

Statistical Errors

The number of events contributing to a single d-distribution has a strong influence on the errors of fit parameter. By combining data of larger time intervals the statistics may be increased at the cost of a loss of sensitivity to fast changes of beam parameters. The results of the fit for different widths of the time interval are available on the World Wide Web [3]. The data samples usually comprise data taking periods between 3-20 hours.

In Figs. 3.1-3.3 it is evident that errors tend to increase with time. This is due to the fact that the data acquisition rate is approximately constant, but the trigger selectivity to pp-elastic events is reduced by about a factor of 5 from the start of the ramp to the top, such that the size of the useful data sample decreases in time by the same factor.

Sources of Systematic Errors

In addition to uncertainties of the fit parameter due to correlation or lack of statistics limitations of the applied model cause systematic errors which are hard to determine quantitatively. As an estimate, the scatter of the fitted values as a function of time for parameters which are known to be constant (e.g. flattop runs, or the vertical target position) can be taken.

The model is known not to account for the following effects:

- the angular resolution in ϕ is a function of ϕ . More precisely, the resolution varies over the width of a so-called “unit-cell” [1], which is formed by the overlap of two adjacent triangular slabs.
- the ϕ resolution varies with z along the slab, simply because the light attenuation introduces larger fluctuations in the number of photoelectrons produced at the cathode of the phototube when the light is produced far away from the lightguide. This is one reason why an attempt to extract information on $\sigma_{x'_b}$ via. Eq. A.18 may fail. In fact an attempt to include $\sigma_{x'_b}$ in the fit lead to values compatible with 0 (within large errors, since the fit is not very sensitive to this parameter) which is not in agreement with Eq. A.19.
- the vertical target position for the CH_2 and C target data samples may differ. The subtracted contribution of quasi-elastic pp events will cause small shifts in the mean value of the d-distribution especially for $|\phi_d| \approx 90°$. However, it is believed that this effect is small.

Summary

Exploiting the fact that pp-elastic Events are coplanar, a measurement of the position where the particles intercept the EDDA detector yields information on the position, width and angle of the COSY beam. The horizontal beam position and the vertical target position can be obtained with an accuracy of about 1mm, beam angles to about 1mrad and the beam width to better than 1mm FWHM (provided the beam is at least 2mm wide).

A Mathematical Description

A.1 Coordinate Systems

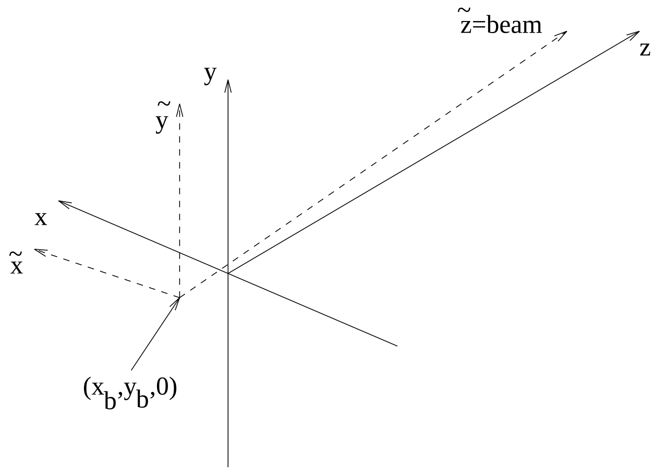

Figure A.1: Sketch of the two coordinate systems

When the beam is both displaced and tilted with respect to the detector it is convenient to introduce a "reaction coordinate system" (RC) ($\tilde{x}$,$\tilde{y}$,$\tilde{z}$) where the reaction vertex is at (0,0,0) and the beam parallel to the $\tilde{z}$-axis. Transformations from the reaction to the EDDA coordinate (EC) system are then described by a rotation by some orthogonal matrix $\mathcal{M}$ followed by a translation to the vertex position (x_b,y_b,0) (we assume the vertex is at z=0, cf. Fig. A.1):

$$\begin{pmatrix} x \\ y \\ z \end{pmatrix} = \begin{pmatrix} x_b \\ y_b \\ 0 \end{pmatrix} + \mathcal{M} \begin{pmatrix} \tilde{x} \\ \tilde{y} \\ \tilde{z} \end{pmatrix} \tag{A.1}$$

The transformation matrix can be derived by expressing the unit vectors $e_{\tilde{x}}$, $e_{\tilde{y}}$, and $e_{\tilde{z}}$of the RC system in the EC space for the case x_b=y_b=0:

- the unit vector in $\tilde{z}$ is given by the beam parameter $x'_b = \mathrm{d}x/\mathrm{d}s$ and $y'_b = \mathrm{d}y/\mathrm{d}s$. If one defines angles θ_x and θ_y via $\tan\theta_x = x'$ and $\tan\theta_y = y'$ on obtains $e_{\tilde{z}} = (\sin\theta_x, \sin\theta_y, k)$, where k is fixed to
$$k = \sqrt{1 - \sin^2\theta_x - \sin^2\theta_y} \tag{A.2}$$
by requiring a length of 1.

- for convenience we choose $e_{\tilde{x}}$ to be in the x-z plane. Orthogonality to $e_{\tilde{z}}$ and unit length fix $e_{\tilde{x}}$ to be $(k/\cos\theta_y, 0, -\sin\theta_x/\cos\theta_y)$.

- $e_{\tilde{y}}$ is then given by the cross product $e_{\tilde{z}} \times e_{\tilde{x}}$.

The transformation matrix is thus given by:

$$\mathcal{M} = \begin{pmatrix} k/\cos\theta_y & -\sin\theta_x\tan\theta_y & \sin\theta_x \\ 0 & \cos\theta_y & \sin\theta_y \\ -\sin\theta_x/\cos\theta_y & -k\tan\theta_y & k \end{pmatrix} \tag{A.3}$$

The inverse transformation is obtained by inverting $\mathcal{M}$. Since $\mathcal{M}$ is orthogonal we simply use the transposed matrix:

$$\begin{pmatrix} \tilde{x} \\ \tilde{y} \\ \tilde{z} \end{pmatrix} = \mathcal{M}^T \begin{pmatrix} x - x_b \\ y - y_b \\ z \end{pmatrix} \tag{A.4}$$

A.2 Dependence of $\bar{d}$ on Beam Parameters

The quantity $\bar{d}$ (as explained in Section 1) is given by

$$\bar{d} \; = -R\cos\frac{\phi_1 - \phi_2}{2} \tag{A.5}$$

and is the *average* d for many events. For a *single* event we need to derive the dependence of the measured ϕ angles (from which d follows) on the final state angles and the beam parameters.

For this purpose we generate a proton-proton elastic event with azimuthal angles $\tilde{\phi}_i$ and polar angles $\tilde{\theta}_i$ in the RC system. The unit vectors of their direction are given by

$$\vec{\tilde{p}_i} = \begin{pmatrix} \sin\tilde{\theta}_i\cos\tilde{\phi}_i \\ \sin\tilde{\theta}_i\sin\tilde{\phi}_i \\ \cos\tilde{\theta}_i \end{pmatrix} \qquad ; i = 1,2 \tag{A.6}$$

We can now calculate the point of interception of the two prongs with the cylindrical slab layer of the EDDA detector at radius R in the EC system viz.

$$\begin{pmatrix} R\cos\phi_i \\ R\sin\phi_i \\ z \end{pmatrix} = \begin{pmatrix} x_b \\ y_b \\ 0 \end{pmatrix} + \lambda\ \mathcal{M}\ \vec{\tilde{p}_i} \qquad ; i = 1,2 \tag{A.7}$$

by determining the three parameters z, ϕ_i (describing the point where the slab layer is hit) and λ. The result can not be obtained analytically, however, for some selected values for x_b, y_b, x'_b, and y'_b the general dependence can be extracted. Therefore, we first approximate the matrix $\mathcal{M}$ for small angles x'_b and y'_b. One obtains:

$$\mathcal{M} = \begin{pmatrix} \sqrt{\frac{1-x_b'^2-y_b'^2}{1-y_b'^2}} & -\frac{x'_b y'_b}{\sqrt{1-y_b'^2}} & x'_b \\ 0 & \sqrt{1-y_b'^2} & y'_b \\ -\frac{x'_b}{\sqrt{1-y_b'^2}} & -y'_b\sqrt{\frac{1-x_b'^2-y_b'^2}{1-y_b'^2}} & \sqrt{1-x_b'^2-y_b'^2} \end{pmatrix} \tag{A.8}$$

We now consider the following cases:

$\boxed{x'_b = y'_b = \mathbf{0}}$:

In this case $\mathcal{M}$ is the unit matrix and we can write:

$$\begin{aligned} R\sin\phi_i - y_b &= z_i \sin\tilde{\phi}_i \tan\tilde{\theta}_i \\ R\cos\phi_i - x_b &= z_i \cos\tilde{\phi}_i \tan\tilde{\theta}_i \end{aligned} \tag{A.9}$$

Dividing both equations and using coplanarity ($\tan\tilde{\phi}_1 = \tan\tilde{\phi}_2$) we can write after some algebra exploiting trigonometric relations:

$$R\cos\frac{\phi_1 - \phi_2}{2} = x_b \cos\frac{\phi_1 + \phi_2}{2} + y_b \sin\frac{\phi_1 + \phi_2}{2} \tag{A.10}$$

which is the same as Eq. 2.3 when applying the sign convention for d and ϕ_d as explained in Section 2.1.

$\boxed{x_b = y_b = y'_b = \mathbf{0}}$:

Here we derive:

$$\begin{aligned} R\cot\phi_i &= \sqrt{1 - {x'_b}^2}\cot\tilde{\phi}_i + \frac{x'_b}{\tan\tilde{\theta}_i \sin\tilde{\phi}_i} \\ \frac{z_i}{R\sin\phi_i} &= x'_b \cot\tilde{\phi}_i + \frac{\sqrt{1 - {x'_b}^2}}{\tan\tilde{\theta}_i \sin\tilde{\phi}_i} \end{aligned} \tag{A.11}$$

from which

$$\sqrt{1 - {x'_b}^2}\cot\phi_i - \frac{x'_b\ z_i}{R\sin\phi_i} = (1 - 2{x'_b}^2)\cot\tilde{\phi}_i \tag{A.12}$$

follows. Coplanarity sets $\cot\tilde{\phi}_1 = \cot\tilde{\phi}_2$ and after some more algebra we obtain:

$$R\cos\frac{\phi_1 - \phi_2}{2} = \frac{x'_b}{\sqrt{1 - {x'_b}^2}}\left\{\frac{z_1 + z_2}{2}\cos\frac{\phi_1 + \phi_2}{2} - \frac{z_1 - z_2}{2}\sin\frac{\phi_1 + \phi_2}{2}\cot\frac{\phi_1 - \phi_2}{2}\right\} \tag{A.13}$$

Keeping only terms linear in x'_b and considering that $\frac{\phi_1 - \phi_2}{2} \approx (2n+1)\frac{\pi}{2}$ for elastic scattering such that the cotangent is close to zero we may write:

$$R\cos\frac{\phi_1 - \phi_2}{2} = x'_b \frac{z_1 + z_2}{2}\cos\frac{\phi_1 + \phi_2}{2} \tag{A.14}$$

Taking the definition of $\bar{d}$ and ϕ_d from Section 2.1 we may now guess the dependence of $\bar{d}$ on x_b, y_b, x'_b, and y'_b:

$$\bar{d} = (x_b + \frac{z_1 + z_2}{2}x'_b)\cos\phi_d + (y_b + \frac{z_1 + z_2}{2}y'_b)\sin\phi_d \tag{A.15}$$

This result has been checked numerically to be accurate within 0.2mm for reasonable values of beam parameters($|x_b|$, $|y_b| < 10$mm,$|x'_b|$, $|y'_b| < 10$mrad).

A.3 Dependence of σ_d on Beam Parameters

The width of the distribution in d at a given angle ϕ_d is derived simply by using error propagation from Eq. A.15.

$$\begin{aligned} {\sigma_d}^2 = &\left(\frac{\partial\bar{d}}{\partial x_b}\sigma_{x_b}\right)^2 + \left(\frac{\partial\bar{d}}{\partial y_b}\sigma_{y_b}\right)^2 + \left(\frac{\partial\bar{d}}{\partial x'_b}\sigma_{x'_b}\right)^2 + \left(\frac{\partial\bar{d}}{\partial y'_b}\sigma_{y'_b}\right)^2 \\ &+ \left(\frac{\partial\bar{d}}{\partial z_1}\sigma_{z_1}\right)^2 + \left(\frac{\partial\bar{d}}{\partial z_2}\sigma_{z_2}\right)^2 + \left(\frac{\partial\bar{d}}{\partial\phi_d}\sigma_{\phi_d}\right)^2 \end{aligned} \tag{A.16}$$

We derive

$$\begin{aligned} {\sigma_d}^2 &= (\sigma_{x_b}^2 + \frac{(z_1+z_2)^2}{4}\sigma_{x_b'}^2)\cos^2\phi_d + (\sigma_{y_b}^2 + \frac{(z_1+z_2)^2}{4}\sigma_{y_b'}^2)\sin^2\phi_d \\ &+ \left({x_b'}^2\cos^2\phi_d + {y_b'}^2\sin^2\phi_d\right)\frac{\sigma_z^2}{2} \\ &+ \left\{y_b\cos\phi_d - x_b\sin\phi_d + \frac{z_1+z_2}{2}(y_b'\cos\phi_d - x_b'\sin\phi_d)\right\}^2 \sigma_{\phi_d}^2 \end{aligned} \tag{A.17}$$

Where the error in z_1 and z_2 was assumed to be the same. Here, the error of ϕ_d is given by the detector resolution in the azimuth

$$\sigma_{\phi_d} = \frac{\sigma_\phi}{\sqrt{2}} \tag{A.18}$$

Of all these terms only a few really contribute. Considering that x_b, and y_b are of the order mm, x_b', and y_b' of the order mrad, z_i of the order 500mm, σ_z of the order 10mm, and $\sigma_{\phi_d} \approx$ 10mrad, the last two terms are suppressed by two orders of magnitude.

The width in x_b and x_b' are related by the twiss-function β

$$\sigma_{x_b'} = \frac{\sigma x_b}{\beta} \tag{A.19}$$

provided we are at the beam waist. β at TP2 in COSY is of the order of some meters, such that we expect $\sigma_{x_b'}^2/\sigma_{x_b}^2$ and $\sigma_{y_b'}^2/\sigma_{y_b}^2$ to be of the order 10^{-1}. It is thus possible to approximate the dependence of σ_d by

$${\sigma_d}^2 = \sigma_{x_b}^2\cos^2\phi_d + \sigma_{y_b}^2\sin^2\phi_d \tag{A.20}$$

This is only the dependence which enters through the right-hand-side of Eq. A.15. The quantity $\bar{d}$ itself is computed from the azimuthal angles which introduces another error through Eq. 2.2. This modifies Eq. A.20 to:

$${\sigma_d}^2 = \sigma_{x_b}^2\cos^2\phi_d + \sigma_{y_b}^2\sin^2\phi_d + \frac{R^2\sigma_\phi^2}{2} \tag{A.21}$$

where we have used that $\sin\frac{\phi_1-\phi_2}{2} \approx 1$ for coplanar events. This expression, however, is not suitable for a fit. The three parameters are σx_b, σy_b, and σ_ϕ are highly correlated, i.e. a combination of two can mock up the influence of the third. This is easy to see, if one multiplies the last term with $1 = \sin^2\phi_d + \cos^2\phi_d$. The assumption of a perfect angular resolution ($\sigma_\phi = 0$) has the same effect as an increased size of the vertex area both in x and y. For a fiber target as it is in use with EDDA the vertex distribution is very narrow in y (some μm) so that without loss of accuracy σ_{y_b} may be set to 0 and we obtain:

$${\sigma_d}^2 = \sigma_{x_b}^2\cos^2\phi_d + \frac{R^2\sigma_\phi^2}{2} \tag{A.22}$$

with two linearly independent parameters x_b and σ_ϕ.

References

[1] S. Heider, Diplomarbeit, ISKP Universität Bonn, 1995.

[2] F. James, CERN Program Library Long Writeup D506: Minuit Version 94.1, Geneva, 1994.

[3] Data is available on the WWW (World Wide Web),
URL "http://www.iskp.uni-bonn.de/edda/analysis/vertex/top.html".